Dehydration of THF-Water Mixtures Using Zeolite-Incorporated Polymeric Membranes

J. G. Varghese,[1,2] A. A. Kittur,[1,2] M. Y. Kariduraganavar[1,2]

[1]Center of Excellence in Polymer Science, Karnatak University, Dharwad 580 003, India
[2]Department of Chemistry, Karnatak University, Dharwad 580 003, India

ABSTRACT: Using a solution technique, polymeric composite membranes were prepared by the incorporation of NaY zeolite into chitosan. The resulting membranes were tested for pervaporation separation of water–tetrahydrofuran mixtures in a temperature range of 30–50°C. The effect of membrane swelling on the separation performance was studied by varying the water composition in the feed from 5 to 30 mass %. Pervaporation data demonstrated that both flux and selectivity increased simultaneously with increasing zeolite content in the membrane. This was explained on the basis of enhancement of hydrophilicity, selective adsorption, and establishment of molecular sieving action. It was found that both total flux and flux of water are close to each other, suggesting that the developed membranes are highly selective toward water. The membrane containing the highest loading of zeolite exhibited the highest separation selectivity of 2140 with a substantial water flux of 16.88×10^{-2} kg/(m^2 h) at 30°C for 5 mass % of water in the feed. From the temperature dependency of diffusion and permeation data, the Arrhenius activation parameters were estimated. A significant difference was noticed between E_{pw} and E_{pTHF}, E_{Dw} and E_{DTHF} values, signifying that membranes developed with higher loading of zeolite exhibited remarkable separation selectivity toward water. The E_p and E_D values ranged between 11.69 and 21.23, and 11.21 and 20.72 kJ/mol, respectively. All the membranes exhibited positive ΔH_s values, suggesting that the heat of sorption is still dominated by Henry's mode of sorption. © 2008 Wiley Periodicals, Inc. J Appl Polym Sci 111: 2408–2418, 2009

Key words: pervaporation; chitosan; NaY zeolite; diffusion coefficient; activation energy

INTRODUCTION

Pervaporation (PV) is a membrane separation technique involving the partial vaporization of a liquid mixture through a membrane whose downstream side is usually kept under vacuum.[1] It is a viable alternative to conventional energy-intensive technologies such as extractive distillation and azeotropic distillation in liquid mixtures separation because it is economical, safe, and ecofriendly.[2] This can be successfully utilized in separating azeotropic mixtures, close boiling liquids, and isomers and also for the dehydration of volatile organic solvents and thermally sensitive organic compounds, since it can overcome the limitation of vapor–liquid equilibrium.[3–5]

Dehydration of organic solvents such as tetrahydrofuran (THF) is of great importance in the field of organic synthesis. Thus, THF is an industrial solvent and chemical intermediate widely recognized for its unique combination of useful properties such as catalytic hydrogenation of maleic acid, anhydride, furan, etc. Therefore, it is being used on a big scale in chemical industry.[5,6] Water-THF has an azeotropic concentration of 6.7 mass % of water, and hence, the separation of these mixtures by conventional methods such as solvent extraction and rotavapor or by distillation could prove uneconomical.[7,8] Various membrane materials have already been utilized for the selective separation of water from aqueous mixtures of THF. Neel et al.[9] used poly(tetrafluoroethylene)–poly(vinylpyrrolidone) membrane to obtain water/THF separation selectivity of 18.4 and total flux of 0.94 kg/(m^2 h) for 5.7 mass % water in the feed. Nguyen et al.[10] obtained water/THF selectivity of 10.4 and total flux of 0.4 kg/(m^2 h) at 293 K using a poly(acrylonitrile)–poly(vinylpyrrolidone) membrane with 5.9 mass % water in the feed. A selectivity of 1518 was obtained by Oikawa et al.[11] with polyacylhydrazone membrane; its total flux was 0.125 kg/(m^2 h) for 6.7 mass % of water in the feed at 298 K. All these membranes employed in such separation studies often yield compromised values of flux and selectivity because of a trade-off

phenomenon existing between flux and selectivity in PV process. On the other hand, zeolite-incorporated polymeric membranes have demonstrated simultaneous increase of flux and selectivity in addition to high chemical strength and good thermal stability.[12–14]

Chitin is one of the most abundant natural biopolymers on earth and is composed of β-(1→4)-linked-2-acetamido-2-deoxy-β-D-glucose (N-acetylglucosamine). The principle derivative of chitin, i.e., chitosan [poly-β(1→4)-D-glucosamine], is a partially deacetylated polymer and has wide applications in various fields such as medicine, pharmaceutics, paper production, textiles, metal chelation, food additives, antimicrobial agents, adhesives, and other industrial applications.[15,16] Recently, many investigators[17–19] have been directed to chitosan as a PV membrane material because of its high affinity toward water, good film-forming properties, functional groups that can be easily modified, and good mechanical and chemical stability. However, the performance of pure chitosan membrane is not satisfactory at higher concentration of water because of a large free-volume available between the molecular chains.[20,21] Great efforts are therefore being attempted to improve the membranes performance by blending it with other polymers such as polysulfone,[22,23] poly(vinyl alcohol) (PVA),[24] and silk fibroin,[25] or by crosslinking it with glutaraldehyde[22] and sulfosuccinic acid.[26] Similarly, inorganic reinforcement such as incorporation of selective zeolite into chitosan membrane is another way of modification of membrane. For instance, Gao et al.[27] and Chen et al.,[21] respectively, studied the PV separation of hydrophilic zeolite-filled PVA and chitosan membranes for organic-water system. In our previous research work, we have reported hydrophobic zeolite-filled PVA membrane[13] and hydrophilic zeolite-filled sodium alginate membrane[14] for the separation of water–isopropanol mixtures. In the latter membrane, we have succeeded in increasing both separation factor and flux simultaneously, although it was a big challenge in PV process because of a trade-off relationship existing between flux and selectivity.

Keeping this in mind, recently our group developed NaY zeolite-incorporated chitosan membranes, which were subjected to water–isopropanol mixtures. The membrane containing 30 mass % of zeolite showed the highest separation selectivity of 2620 with a substantial flux of 11.50×10^{-2} kg/(m² h) at 30°C for 5 mass % of water in the feed. It was demonstrated that both flux and selectivity increased simultaneously with increasing zeolite content in the membrane. This has prompted us to extend the study of these membranes for the separation of water-THF mixtures. We report here the experimental results of permeation flux, separation selectivity, and diffusion coefficients at different temperatures. The morphology of the membranes was characterized by scanning electron microscopy (SEM). The diffusion coefficients have been calculated from the Fick's diffusion equation. From the temperature dependency of permeation flux and diffusion coefficients data, the Arrhenius activation parameters have been estimated. These results are discussed in terms of PV separation efficiency of the membranes.

EXPERIMENTAL

Materials

Chitosan (average molecular weight 200,000; N-deacetylation degree 75–85%) was obtained from Sigma-Aldrich Chemicals, USA. THF and acetic acid (HAc) were purchased, respectively, from Ranbaxy Fine Chemicals, New Delhi, India, and S.D. Fine Chemicals, Mumbai, India. NaY zeolite was kindly supplied by Indian Petrochemicals, Baroda, India. All the chemicals were of reagent grade and were used without further purification. Double distilled water was used throughout the research work. The characteristic properties of NaY zeolite are given in Table I.

Membrane preparation

Chitosan (3 g) was dissolved in 100 mL of deaerated-distilled water containing 2% of acetic acid under constant stirring for about 24 h at room temperature. The solution was then filtered through a fritted glass disc filter to remove undissolved residue particles and the filtrate was left overnight to release the effervescence. The resulting homogeneous solution was spread onto a glass plate with the aid of a casting knife in a dust-free atmosphere at room temperature. After being dried for about 48 h, the membrane was subsequently peeled-off and was designated as M-1.

To prepare zeolite-incorporated chitosan membrane, a known amount of NaY zeolite was added into a chitosan solution. The amount of chitosan was

TABLE I
Physicochemical Properties of Hydrophilic NaY Zeolite[28,29]

Counter ion	Na$^+$
SiO$_2$/Al$_2$O$_3$	2.6
Density	1.27 g/mL
Pore size	0.5–2.0 μm
Pore volume	0.47 mL/g
Topology	FAU
Nature	Hydrophilic

kept constant for each membrane. The mixed solution was stirred for about 24 h, followed by sonication for about 30 min at a fixed frequency of 38 kHz (grant XB6, UK) to break the aggregated crystals of zeolite and so as to improve the dispersion of zeolite in the polymer matrix. It was then filtered and left overnight to obtain a homogeneous solution. The resultant solution was poured onto a glass plate and the membrane was dried as mentioned above. The amount of NaY zeolite with respect to chitosan was varied as 10, 20, 30, and 40 mass %, and the membranes thus obtained were designated as M-2, M-3, M-4, and M-5, respectively. The thickness of these membranes was measured at different points using a Peacock dial thickness gauge (model G; Ozaki, Japan) with an accuracy of ± 2 μm and the average thickness was considered for the calculation. Thickness of these membranes was found to be 40 $\pm$ 2 μm. Except characterization of membrane morphology, the physical and spectroscopic properties of the derivatized membranes were described in our previous paper.[12]

Scanning electron microscopy

The morphology of the pure chitosan and its zeolite-incorporated membranes was investigated at 10 kV using a JSM-840A SEM (Jeol, Tokyo, Japan). All the specimens were coated with a conductive layer (400 Å) of sputtered gold.

Swelling measurement

The degree of membranes swelling was performed with different compositions of water-THF mixtures using an electronically controlled oven (WTB Binder, Jena, Germany). The masses of the dry membranes were first determined and these were equilibrated by immersing in different compositions of the feed mixtures in sealed vessels at 30°C for 24 h. The swollen membranes were weighed as quickly as possible after careful blotting on a digital microbalance (model B204-S; Mettler-Toledo International, Zurich, Switzerland) having a sensitivity of ± 0.01 mg. The percent degree of swelling (DS) was calculated as

$$DS(\%) = \left(\frac{W_s - W_d}{W_d}\right) \times 100 \tag{1}$$

where W_s and W_d are the masses of the swollen and dry membranes, respectively.

PV experiment

PV experiments were carried out using an indigenously designed apparatus reported in our previous articles.[14,30] The effective area of the membrane in contact with the feed mixture was 34.23 cm^2 and the capacity of the feed compartment was about 250 cm^3. The vacuum in the down streamside of the PV cell was maintained [1.333224 $\times$ 10^3 Pa (10 Torr)] using a two-stage vacuum pump (Toshniwal, Chennai, India). The test membrane was allowed to equilibrate for about 2 h while in contact with the feed mixture before performing the experiment. After attaining a steady state, the permeate was collected in a trap immersed in liquid nitrogen jar on the downstream side of the PV cell at fixed time intervals. The experiments were carried out at 30, 40, and 50°C. The water composition in the feed was varied from 5 to 30 mass %. The obtained permeate was weighed on a digital microbalance to determine the flux. The compositions of water and THF were estimated by measuring the refractive index of the mixture within an accuracy of ± 0.0001 units using Abbe's refractometer (Atago-3T, Tokyo, Japan) and by comparing it with a standard graph of refractive index, which was established with the known compositions of water/THF mixtures. All the experiments were performed at least three times and the results were averaged. The results of permeation for water-THF mixtures during the PV were reproducible within the admissible range.

The membrane efficiency in PV experiments was evaluated by calculating the total flux (J), separation factor (α_{sep}), and PV separation index (PSI). These were calculated, respectively, using the following equations:

$$J = \frac{W}{At} \tag{2}$$

$$\alpha_{sep} = \frac{P_w/P_{THF}}{F_w/F_{THF}} \tag{3}$$

$$PSI = J(\alpha_{sep} - 1) \tag{4}$$

where W represents the mass of permeate (kg); A is the effective membrane area (m^2); t is the permeation time (h); P and F are the mass percent of permeate and feed, respectively; subscripts w and "THF" denote water and THF, respectively.

RESULTS AND DISCUSSION

Scanning electron microscopy

Figure 1 illustrates the SEM photographs of the surface and cross-sectional views of the pure chitosan and its NaY zeolite incorporated membranes. From the micrographs, it is confirmed that the distribution of NaY zeolite increased from membrane M-2 to M-5 with increasing zeolite content. Except in membrane M-5, the zeolite was evenly dispersed throughout the membrane matrix with no apparent
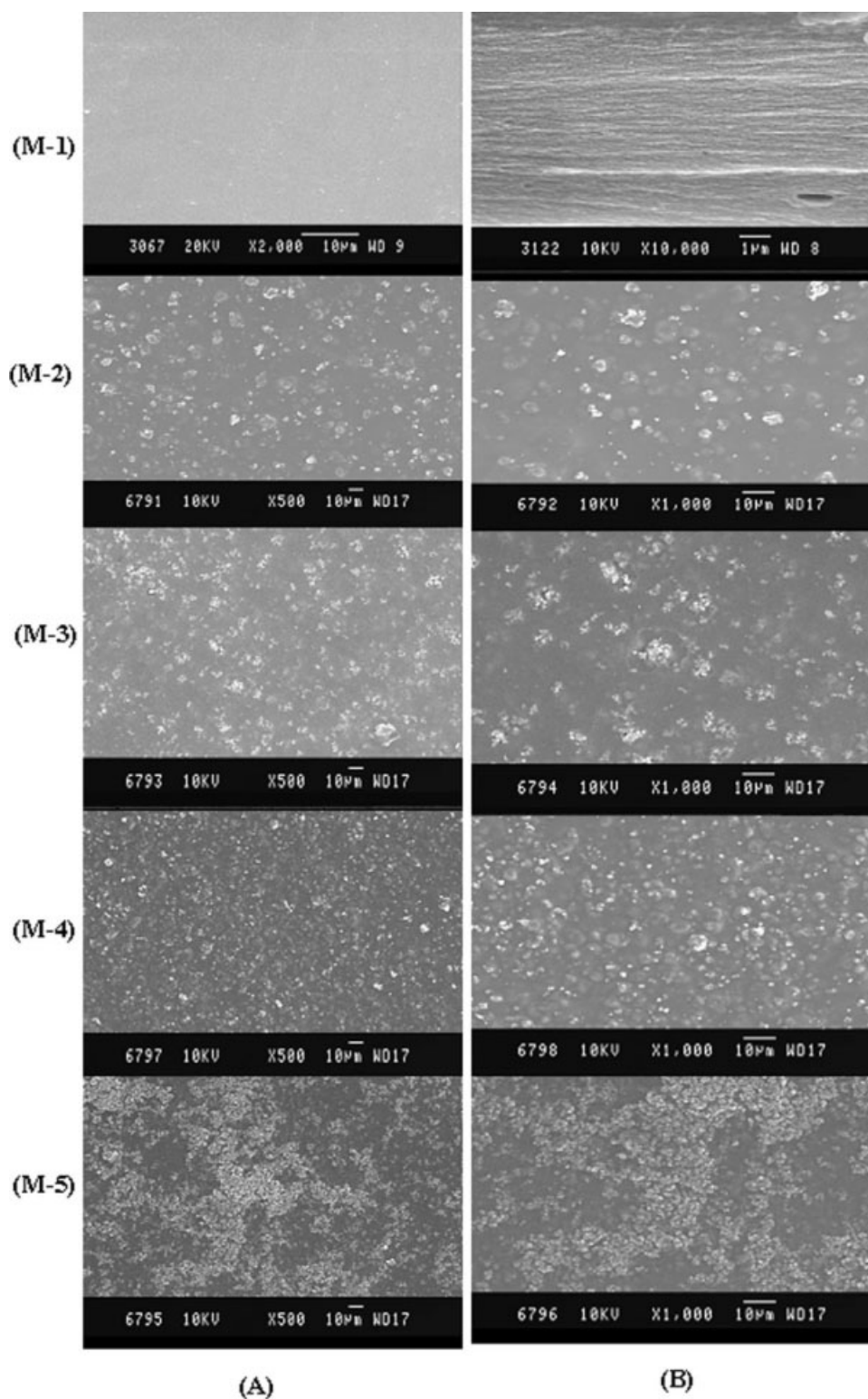
Figure 1 SEM micrographs of pure chitosan and its zeolite-incorporated membranes: (A) surface views and (B) cross-sectional views.

clustering. This ensures that the zeolite incorporated membranes developed here are free from possible defects. However, we can notice the clustering of zeolite in the micrographs of M-5 and it is expected owing to higher loading of zeolite.

Effects of feed composition and zeolite loading on membrane swelling

Membrane swelling in certain liquids depends on the chemical composition and microstructure of the polymer and the incorporated moieties, which
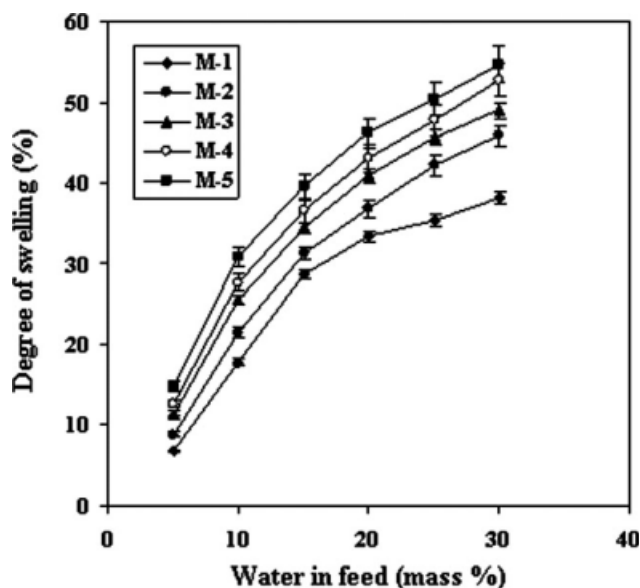
Figure 2 Variation of degree of swelling with different mass % of water in the feed for pure chitosan and its zeolite-incorporated membranes.

strongly influence the sorption mechanism.[31] Membrane swelling is one of the important factors in PV process, as it controls the transport of permeating molecules under the chemical potential gradient.

To study the effects of feed composition and zeolite loading on the membrane swelling, the percent degree of swelling of all membranes was plotted with respect to different mass % of water in the feed at 30°C as shown in Figure 2. It is evident from the plot that the degree of swelling increased monotonously for all the membranes with increasing mass % of water in the feed. This is attributed to strong interactions occurring between water molecules and the membrane containing —NH_2, —NH_3^+, —OH groups, and Na^+ ions. As the water concentration increases in the feed, the interaction with water becomes more predominant, given that water causes a greater degree of swelling than that of THF with the membranes. However, in case of pure chitosan membrane, the degree of swelling appears to be constant at higher concentration of water. This is an indicative of decreased solubility of penetrants in the membrane because of an attainment of saturation of hydrophilic groups present in the membrane matrix. This situation is not same with the zeolite-incorporated membranes, wherein incorporated zeolite enhances the hydrophilic character of the membranes. Thus, the degree of swelling exhibits a steep increase at higher concentration of water in the feed.

On the other hand, the degree of membranes swelling enhanced considerably than that of a pure membrane, when the polymer matrices are filled with NaY zeolite. This is mainly because of hydro-

philic nature of the incorporated NaY zeolite in the membrane matrix. Besides, the incorporated NaY zeolite contains Na^+ ions in its channels, which tend to enhance the electrostatic force of attraction between water molecules and the membrane. Thus, these combined properties substantially increase the adsorption of water molecules, resulting in greater degree of swelling with increasing zeolite content in the membrane.

Effects of feed composition and zeolite loading on PV

To study the effects of feed composition and zeolite loading on the permeation, the total permeation flux was plotted for all the membranes as a function of different mass % of water in the feed, as shown in Figure 3. It is observed that the total permeation flux increased monotonously for all the zeolite-incorporated membranes with increasing water concentration in the feed, attributed to an increased selective interaction between water molecules and the zeolite-incorporated membranes. However, for pure membrane (M-1), the permeation flux increased upto 15 mass % of water in the feed, and beyond this, the permeation flux becomes almost constant. This may be the result of attaining the saturation of interactive groups (NH_2, NH_3^+, OH) of chitosan with increasing water concentration in the feed. However, this phenomenon does not occur with the zeolite-incorporated chitosan membranes, wherein the content of NaY zeolite enhances the selective interactions between water molecules and the membrane. This is mainly attributed to a combined
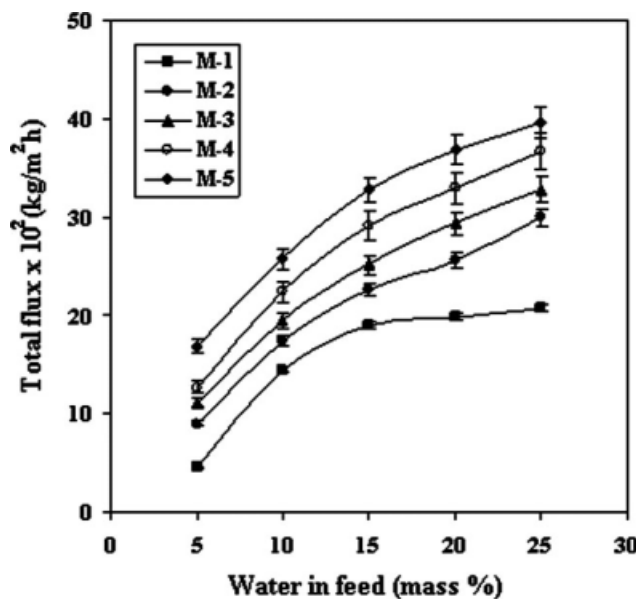

Figure 3 Variation of total flux with different mass % of water in the feed for pure chitosan and its zeolite-incorporated membranes.
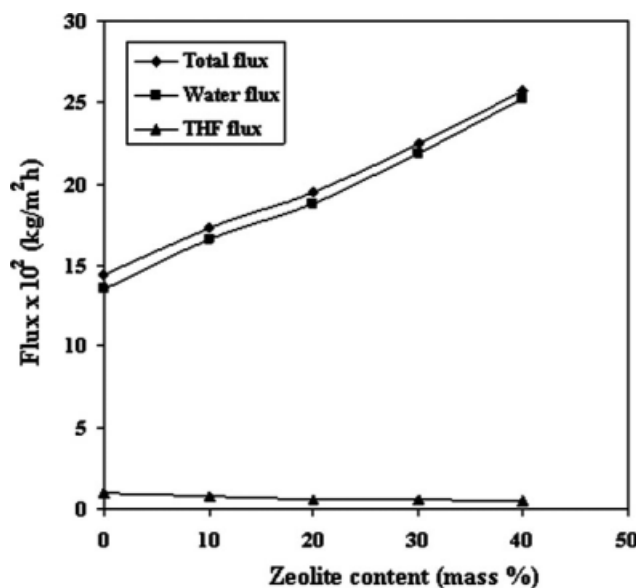
Figure 4 Variation of total flux, fluxes of water and THF with different mass % of zeolite-incorporated chitosan membranes at 10 mass % of water in the feed.

influence of ionic species (Na^+) present in the zeolite cages and porous nature of zeolite, apart from its hydrophilic nature.[12] These together are responsible for the higher permeation flux with increasing water concentration in the feed.

In the PV process, the efficiency of the membrane is generally assessed on the basis of permeation of individual components. Therefore, the extent of permeation of individual components was determined by plotting the total flux and fluxes of water and THF as a function of zeolite content in the membrane for 10 mass % of water in the feed as shown in the Figure 4. From the plot, it is clear that the total flux and flux of water are close to each other whereas the flux of THF is negligibly small for all the membranes throughout the investigated range of water composition, indicating that the membranes developed in the present study are highly water selective. Further, when we view the plot carefully, it is noticed that the difference between the total flux and water flux becomes insignificant with increasing zeolite content in the membrane matrix, and as a result, the flux of THF was declined from membrane M-1 to M-5. This clearly reveals that the amount of zeolite incorporated in the membranes effectively improves the membranes' efficiency, thereby enhancing selective transport.

The overall selectivity of a membrane in PV process is generally described on the basis of interaction between the membrane and permeating molecules, molecular size of the permeating species, and pore diameter of the membrane. Figure 5 demonstrates the influence of water composition on the selectivity of all membranes. It is observed that the selectivity
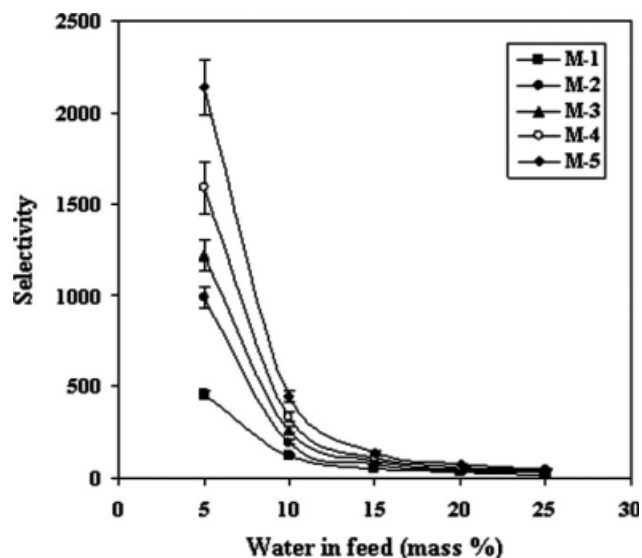

Figure 5 Variation of separation selectivity with different mass % of water in the feed for pure chitosan and its zeolite-incorporated membranes.

of all the membranes decreased drastically from 5 to 10 mass % of water and then it decreased gradually upon further increasing the water concentration in the feed. At higher concentration of water, the membrane swells greatly because of an establishment of strong interaction between the membrane and water molecules, thereby suppressing the interaction between NaY zeolite and chitosan within the membrane material. This in turn may be the reason for the development of very minute narrow openings at the interface between the zeolite and chitosan.[21] This allows the THF molecules to pass through the membrane along with the water molecules. Therefore, the selectivity underwent a drastic decrease at higher
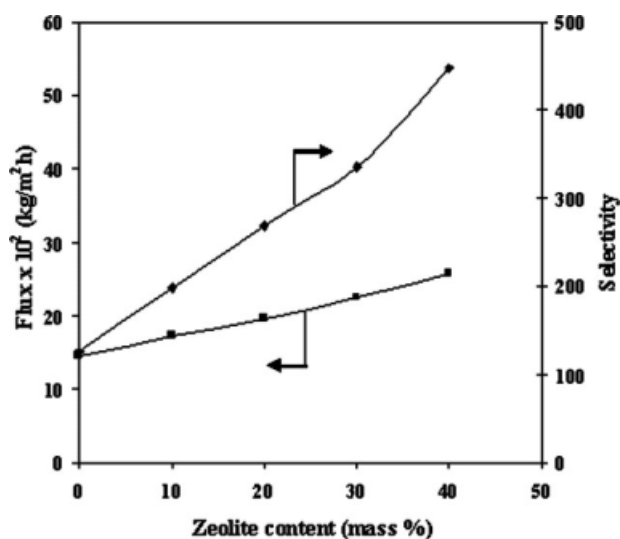

Figure 6 Variation of total flux and selectivity with different mass % of zeolite-incorporated chitosan membranes at 10 mass % of water in the feed.

TABLE II
Pervaporation Flux and Separation Selectivity Data of Different Membranes Measured at 30°C for Different Mass % of Water in the Feed

Mass % of water	J [$\times 10^2$ kg/(m² h)]					α_{sep}				
	M-1	M-2	M-3	M-4	M-5	M-1	M-2	M-3	M-4	M-5
5	4.55	8.98	10.27	12.67	16.88	455	986	1223	1591	2140
10	14.45	17.29	19.45	22.41	25.73	126	198	268	335	448
15	18.90	22.68	25.19	29.21	32.81	54	83	97	116	143
20	19.84	25.67	29.42	32.98	36.85	34	48	56	66	76
25	20.70	30.00	32.87	36.74	39.64	18	31	35	43	53

concentration of water in the feed, irrespective of the amount of zeolite loading in the membrane.

On the other hand, there was a tremendous enhancement in the selectivity from membrane M-1 to M-5, upon increasing the amount of zeolite in the membrane. This can be clearly observed from the Figure 6, which shows the variation of flux and selectivity as a function of zeolite content in the membrane at 10 mass % of water in the feed. Generally, with increasing packing density or by incorporating the zeolite in the polymer matrix, permeation flux decreases and selectivity increases.[13,32] However, in the present study, both the permeation flux and selectivity increased simultaneously with increasing zeolite content in the membrane. Although this is in contrast to a trade-off phenomenon existing between flux and separation factor in the PV process, a significant enhancement of hydrophilicity, selective adsorption and establishment of molecular sieving action by the creation of pores in the membrane matrix were achieved by incorporating porous zeolite in the polymer matrix. This can be further explained in such a way that when we use water selective zeolite-incorporated membranes, the transport of water molecules through the membrane occurs in a straight path through the zeolite pores with subsequent adsorption at the feed side followed by desorption at the permeate side, which in turn is responsible for higher water flux. If sufficient water is available inside the membrane, then the zeolite pores will be largely occupied by these water molecules, preventing the THF molecules from entering the zeolite pores. Thus, on their way through the membrane the THF molecules have to

move around the zeolite pores. The higher water concentration inside the membrane close to the permeate side of the membrane and the fact that water can travel along the straight path whereas THF has to follow a more tortuous path, in which the membrane act together in explaining the way in which membrane performance is enhanced, both in terms of flux and selectivity when zeolite is incorporated into the membrane matrix.[33]

The results of total flux and selectivity and the fluxes of water and THF measured at 30°C for all the membranes in the investigated feed compositions are presented in the Tables II and III, respectively. It is observed that there is a systematic increase of total flux and flux of water with increasing the amount of zeolite and feed composition. Although the flux of THF increased with increasing water composition, it decreased with increasing the amount of zeolite as expected. Similarly, the selectivity increased systematically with increasing the amount of zeolite throughout the investigated range of water composition, indicating that the addition of zeolite increases the selectivity of the membrane.

Effect of zeolite loading on pervaporation separation index

Pervaporation separation index (PSI) is the product of total permeation and separation factor, which characterizes the membrane separation ability. Therefore, this index can be used as a relative guideline for designing the new membranes for PV applications. Figure 7 shows the variation of PSI as a function of zeolite content in the membrane for 10

TABLE III
Pervaporation Fluxes of Water and Tetrahydrofuran of Different Membranes Measured at 30°C for Different Mass % of Water in the Feed

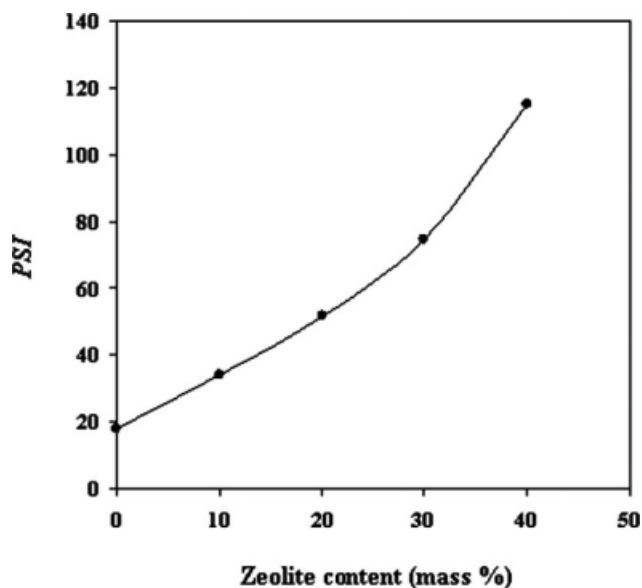| Mass % of water	J_w [$\times 10^2$ kg/(m² h)]					J_{THF} [$\times 10^3$ kg/(m² h)]				
	M-1	M-2	M-3	M-4	M-5	M-1	M-2	M-3	M-4	M-5
5	4.37	8.81	10.11	12.52	16.74	1.83	1.70	1.57	1.50	1.49
10	13.49	16.54	18.82	21.82	25.22	9.61	7.52	6.32	5.87	5.07
15	17.12	21.23	23.80	27.84	31.56	17.80	14.50	13.90	13.70	12.50
20	17.75	23.71	27.47	31.08	35.01	20.90	19.60	19.50	19.00	18.40
25	17.80	27.36	30.26	34.32	37.53	29.00	26.40	26.10	24.20	21.10

Figure 7 Variation of pervaporation separation index with different mass % of zeolite-incorporated chitosan membranes at 10 mass % of water in the feed.

mass % of water in the feed at 30°C. It is observed that PSI values increased exponentially with increasing the zeolite content in the membrane. This in turn specifies that the membranes having higher amount of zeolite exhibit better efficiency for the separation of THF-water mixtures. This is mainly because of the incorporation of zeolite into the polymer matrix that changes not only the hydrophilicity of the membrane but also its structure, which may have a significant influence on the process of diffusion. Sorption is only the first step, and in the second step of diffusion, unique properties of zeolite and their significant role in the membrane matrix enhances the overall performance of the membranes.

Diffusion coefficient

Mass transport of binary liquid molecules in PV experiments is generally explained by the solution-diffusion mechanism, which occurs in three steps: sorption, diffusion, and evaporation.[34] Thus, the permeation rates and selectivity are governed by the solubility and diffu-

sivity of each component of the feed mixture to be separated. In PV process, because of the establishment of fast equilibrium distribution between the bulk feed and upstream surface of the membrane, the diffusion step controls the migration of the penetrants.[13,35] Therefore, it is important to estimate the diffusion coefficient, D_i of penetrating molecules to understand the mechanism of molecular transport.

From Fick's law of diffusion, the diffusion flux can be expressed as[36]

$$J_i = -D_i \frac{dC_i}{dx} \tag{5}$$

where J is the permeation flux per unit area [kg/(m² s)], D is the diffusion coefficient (m²/s), C is the concentration of permeate (kg/m³), subscript i stands for water or THF, and x is the diffusion length (m). For convenience, it is assumed that the concentration profile along the diffusion length is linear. Therefore, the diffusion coefficient can be calculated using the following equation[37]:

$$D_i = \frac{J_i \delta}{C_i} \tag{6}$$

where δ is the membrane thickness. The calculated values of D_i at 30°C are presented in Table IV. It is observed that the diffusion coefficients of water increased systematically from membrane M-1 to M-5 while suppressing the diffusion coefficients of THF. It clearly indicates that the membranes prepared in the present study are of remarkable separation ability for the separation of water-THF mixtures especially at lower concentration of water in the feed (azeotropic point). This is because the incorporation of zeolite in the polymer matrix establishes straight and tortuous paths for water and THF, respectively. On the other hand, with increasing the water concentration in the feed for all the membranes, the diffusion coefficients of water decreases while increasing the diffusion coefficients of THF. This is expected because of decrease in membrane selectivity as described in PV study owing to the formation of tiny cracks at the interface between the NaY

TABLE IV
Diffusion Coefficients of Water and Tetrahydrofuran Calculated at 30°C from Eq. (6) for Different Membranes at Different Mass % of Water in the Feed

Mass % of water	D_w ($\times 10^8$ cm²/s)					D_{THF} ($\times 10^9$ cm²/s)				
	M-1	M-2	M-3	M-4	M-5	M-1	M-2	M-3	M-4	M-5
5	30.00	37.50	43.50	54.80	75.60	1.54	1.43	1.33	1.26	1.25
10	28.30	35.10	40.20	47.20	55.20	8.56	6.70	5.63	5.23	4.51
15	23.70	29.70	33.60	39.70	45.30	16.80	13.70	13.10	12.90	11.80
20	18.30	24.70	28.80	32.80	37.20	21.00	19.60	19.60	19.00	18.50
25	14.60	22.70	25.30	28.80	31.60	31.00	28.20	28.00	25.90	22.50

TABLE V
Pervaporation Flux and Separation Selectivity of Different Membranes Measured at Different Temperatures for 10 Mass % of Water in the Feed

Temp. (°C)	J [$\times 10^2$ kg/(m^2 h)]					α_{sep}				
	M-1	M-2	M-3	M-4	M-5	M-1	M-2	M-3	M-4	M-5
30	14.45	17.29	19.45	22.41	25.73	126	198	268	335	448
40	18.06	20.10	21.92	24.48	28.29	70	81	116	131	162
50	24.63	26.16	27.82	30.43	34.34	54	67	81	102	114

zeolite and chitosan in the polymer matrix at higher composition of water in the feed.

Effect of temperature on membrane performance

The effect of operating temperature on PV performance was studied for all the membranes at 10 mass % of water in the feed and the resulting values are displayed in Table V. It is observed that the permeation rate was found to increase from 30 to 50°C for all the membranes, while decreasing the separation selectivity. This is because of decreased interaction between permeates, permeants, and membrane at higher temperature, which increases the plasticizing action of the permeates.[12] Therefore, the permeation of diffusing molecules and the associated molecules through the membranes becomes easier, resulting in an increase of total permeation flux, while suppressing the selectivity. This effect prompted us to estimate the activation energy for permeation and diffusion using the Arrhenius-type equation[38]:

$$X = X_o \exp\left(\frac{-E_x}{RT}\right) \quad (7)$$

where X represents permeation (J) or diffusion (D), X_o is a constant representing the preexponential fac-tor J_o or D_o, E_x represents activation energy for permeation or diffusion depending on the transport process under consideration, and RT is the usual energy term. As the temperature increases, the vapor pressure in the feed compartment also increases, but the vapor pressure at the permeate side is unaffected. This in turn results to increase in driving force with increasing temperature.

Arrhenius plots are shown in Figures 8 and 9 for the temperature dependence of permeation flux and diffusion, respectively. In both the cases, linear behavior was observed, signifying that permeation flux and diffusivity follow the Arrhenius trend. From least-squares fits of these linear plots, the activation energy values for permeability (E_p) and diffusivity (E_D) were estimated and the results thus obtained are presented in Table VI. Similarly, we have also estimated the activation energy values for permeation of water (E_{pw}) and THF (E_{pTHF}), and diffusion of water (E_{Dw}) and THF (E_{DTHF}), but the plots are not given to avoid the crowdness. The values thus obtained are included in Table VI. It is noticed that a pure membrane (M-1) exhibits higher E_p and E_D values compared to those of zeolite-incorporated membranes (M-2 to M-5). This suggests that both permeating and diffusing molecules require
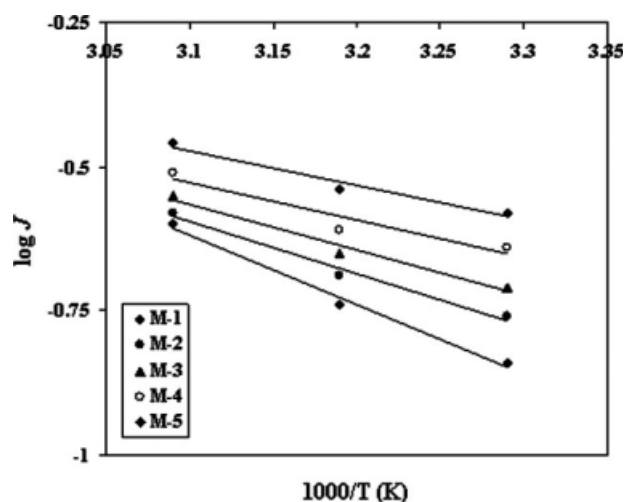

Figure 8 Variation of log J with temperature for different mass % of zeolite-incorporated chitosan membranes at 10 mass % of water in the feed.

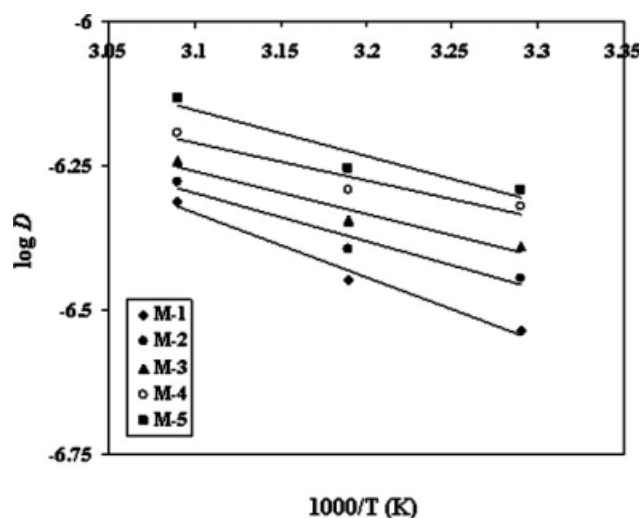**Figure 9** Variation of log D with temperature for different mass % of zeolite-incorporated chitosan membranes at 10 mass % of water in the feed.

TABLE VI
Arrhenius Activation Parameters for Permeation and Diffusion, and Heat of Sorption

Parameters (kJ/mol)	M-1	M-2	M-3	M-4	M-5
E_p	21.23	16.81	14.52	12.40	11.69
E_{pw}	18.13	13.48	11.57	10.03	8.94
E_{pTHF}	53.30	57.78	58.74	60.46	65.36
E_D	20.72	15.83	13.78	11.88	11.21
E_{Dw}	19.19	14.41	12.56	10.90	10.42
E_{Do}	53.27	57.73	58.72	60.52	65.49
ΔH_S	0.51	0.98	0.74	0.52	0.48

more energy for transport through the pure membrane (M-1) because of its dense nature. Obviously, zeolite incorporated membranes consume less energy because of the establishment of molecular sieving action attributed to the presence of sodalite and super cages in the framework of zeolite.[12] As a result, the activation energies for permeation and diffusion decreased systematically from membrane M-2 to M-5 with increasing zeolite content.

On the other hand, a large difference was noticed between E_{pw} and E_{pTHF} values. However, the difference is more significant particularly for the membranes having higher loading of zeolite, exhibiting remarkable separation selectivity toward water. A similar situation was also noticed between E_{Dw} and E_{DTHF} values, justifying the explanation.

Although E_p values are higher than those of E_D values in all the membranes, the difference is not significant, indicating that both permeation and diffusion almost equally contribute to the PV process. The E_p and E_D values ranged between 11.69 and 21.23, and 11.21 and 20.72 kJ/mol, respectively. Using these values, we have calculated the heat of sorption as

$$\Delta H_s = E_p - E_D \qquad (8)$$

The resulting ΔH_s values are included in Table VI. The ΔH_s values provide the additional information about the transport of molecules through the polymer matrix. It is a composite parameter involving contribution of both Henry's and Langmuir's type of sorption.[39] Henry's mode requires both the formation of a site and the dissolution of the species into that site. The formation of a site involves an endothermic contribution to the sorption process. In case of Langmuir's mode, the site already exists in the polymer matrix, and consequently, sorption by hole filling yields more exothermic heats of sorption. In the present study, the ΔH_s values obtained are positive for all the membranes, suggesting that Henry's sorption is still predominant, giving an endothermic contribution.

CONCLUSIONS

Using a solution technique, NaY zeolite-incorporated chitosan membranes were prepared and successfully employed for the separation of water-THF mixtures. An increase of zeolite content in the membrane results to a simultaneous increase of both permeation flux and selectivity. This was explained on the basis of significant enhancement of hydrophilic character, selective adsorption and establishment of molecular sieving action including a reduction of pore size of the polymer matrix. While assessing the membranes' efficiency, it was clearly noticed that both total flux and flux of water are close to each other, signifying that the membranes developed in the present study by the incorporation of zeolite are highly selective toward water. The PV separation index data also indicated that the higher the loading of zeolite, the better is the membranes performance. The highest separation selectivity was found to be 2140 with a flux of 16.88×10^{-2} kg/(m^2 h) for the membrane with the highest loading of zeolite at 30°C for 5 mass % of water in the feed. With regard to temperature effect, the permeation rate was found to increase, while suppressing the selectivity. This was attributed to decreased interaction between permeating molecules, permeants, and membrane at higher temperature.

A significant difference was noticed between E_{pw} and E_{pTHF}, and E_{Dw} and E_{DTHF} values. In addition to this, the difference was more significant particularly for the membranes having higher loading of zeolite, suggesting that membranes developed with higher loading of zeolite exhibited remarkable separation selectivity toward water.

The E_p and E_D values ranged between 11.69 and 21.23, and 11.21 and 20.72 kJ/mol, respectively. The zeolite incorporated membranes exhibited lower activation energy compared to that of a pure membrane, indicating that the permeants require less energy during the process because of molecular sieving action attributed to the presence of sodalite and super cages in the framework of zeolite. The almost equal magnitude of E_p and E_D values suggests that both permeation and diffusion contribute equally to the PV process. For all the membranes, Henry's mode of sorption dominates the process, giving an endothermic contribution.

References

1. Neel, J. In Pervaporation Membrane Separation Processes; Huang R. Y. M., Ed.; Elsevier: Amsterdam, 1994; p 1.
2. Smitha, B.; Suhanya, D.; Sridhar, S.; Ramakrishna, M. J Membr Sci 2004, 241, 1.

3. Potts, J. E. Kirk-Othmer Encyclopedia of Chemical Technology, 3rd ed.; Wiley-Interscience: New York, 1984.

4. Baker, R. W.; Cussler, E. L.; Eykamp, W.; Koros, W. J.; Riley, R. L.; Strathmann, H. Membrane separation systems recent developments and future directions; Noyes Data Corp: Park Ridge, NJ, 1991.

5. Chapman, P. D.; Tan, X.; Livingston, A. G.; Li, K.; Oliveira, T. J Membr Sci 2006, 268, 13.

6. Riddick, J. A.; Bunger, W. B. In Organic Solvents, 3rd ed.; Wiley-Interscience: New York, 1970; p 857.

7. Shiguang, L.; Tuan, V. A.; Noble, R. D.; Falconer, J. L. Ind Eng Chem Res 2001, 40, 4577.

8. Xu, S.; Wang, H. Chem Eng Res Des 2006, 84, 478.

9. Neel, J.; Nguyen, Q. T.; Clement, R.; Blanc, L. L. J Membr Sci 1983, 15, 43.

10. Nguyen, Q. T.; Blanc, L. L.; Neel, J. J Membr Sci 1985, 22, 245.

11. Oikawa, E.; Tamura, S.; Arai, Y.; Aoki, T. J Appl Polym Sci 1995, 58, 1205.

12. Kittur, A. A.; Kulkarni, S. S.; Aralaguppi, M. I.; Kariduraganavar, M. Y. J Membr Sci 2005, 247, 75.

13. Kittur, A. A.; Kariduraganavar, M. Y.; Toti, U. S.; Ramesh, K.; Aminabhavi, T. M. J Appl Polym Sci 2003, 90, 2441.

14. Kariduraganavar, M. Y.; Kittur, A. A.; Kulkarni, S. S.; Ramesh, K. J Membr Sci 2004, 238, 165.

15. Welsh, E. R.; Schauer, C. L.; Qadri, S. B.; Price, R. R. Biomacromolecules 2002, 3, 1370.

16. Welsh, E. R.; Price, R. R. Biomacromolecules 2003, 4, 1357.

17. Uragami, T.; Matsuda, T.; Okuno, H.; Miyata, T. J Membr Sci 1994, 88, 243.

18. Uragami, T.; Kato, S.; Miyata, T. J Membr Sci 1997, 124, 203.

19. Nawawi, M.; Ghazali, M.; Huang, R. Y. M. J Membr Sci 1997, 124, 53.

20. Li, W. J.; Pan, W. S.; Tang, Y. Chem J Chin Uni 1992, 3, 415.

21. Chen, X.; Yang, H.; Gu, Z.; Shao, Z. J Appl Polym Sci 2001, 79, 1144.

22. Huang, R. Y. M.; Pal, R.; Moon, G. Y. J Membr Sci 1999, 160, 17.

23. Feng, X.; Huang, R. Y. M. J Membr Sci 1996, 116, 67.

24. Tang, Y.; Zhao, H.; Li, W. Funct Polym 1992, 5, 1.

25. Chen, X.; Li, W.; Shao, Z.; Zhong, W.; Yu, T. J Appl Polym Sci 1999, 73, 975.

26. Jegal, J.; Lee, K. H. J Appl Polym Sci 1999, 71, 671.

27. Gao, Z.; Yue, Y.; Li, W. Zeo 1996, 16, 70.

28. Vankelecom, I. F. J.; Beukelaer, S. D.; Uytterhoeven, J. B. J Phys Chem B 1997, 101, 5186.

29. Vankelecom, I. F. J.; Dotremont, C.; Morobe, M.; Uytterhoeven, J. B.; Vandecasteele, C. J Phys Chem B 1997, 101, 2154.

30. Kariduraganavar, M. Y.; Kulkarni, S. S.; Kittur, A. A. J Membr Sci 2005, 246, 83.

31. Kittur, A. A.; Tambe, S. M.; Kulkarni, S. S.; Kariduraganavar, M. Y. J Appl Polym Sci 2004, 94, 2101.

32. Kurkuri, M. D.; Toti, U. S.; Aminabhavi, T. M. J Appl Polym Sci 2002, 86, 3642.

33. te Hennepe, H. J. C.; Bargeman, D.; Mulder, M. H. V.; Smolders, C. A. J Membr Sci 1987, 35, 39.

34. Lee, Y. M.; Bourgeois, D.; Belfort, G. J Membr Sci 1989, 44, 161.

35. Hwang, S. T.; Kammermeyer, K. Membrane in Separations; Wiley-Interscience: New York, 1975.

36. Yamasaki, A.; Iwatsubo, T.; Masuoka, T.; Misoguchi, K. J Membr Sci 1994, 89, 111.

37. Kusumocahyo, S. P.; Sudoh, M. J Membr Sci 1999, 161, 77.

38. Huang, R. Y. M.; Yeom, C. K. J Membr Sci 1998, 58, 33.

39. Weinkauf, D. H.; Paul, D. R. In Barrier Polymers and Structures (ACS Symposium Series 423); Koros, W. J., Ed.; American Chemical Society: Washington, DC, 1990; p 60.